MOLECULAR ECOLOGY

Molecular Ecology (2014) **23**, 1457–1472 doi: 10.1111/mec.12439

SPECIAL ISSUE: NATURE'S MICROBIOME

Ontogenetic variation in epibiont community structure in the deep-sea yeti crab, *Kiwa puravida*: convergence among crustaceans

SHANA K. GOFFREDI,* ANN GREGORY,* WILLIAM J. JONES,† NORMA M. MORELLA* and REID I. SAKAMOTO*

Biology Department, Occidental College, Los Angeles, CA 90041, USA, †Environmental Genomics Core Facility, Environmental Health Sciences, University of South Carolina, Columbia, SC 29208, USA

Abstract

Recent investigations have demonstrated that unusually 'hairy' yeti crabs within the family Kiwaidae associate with two predominant filamentous bacterial families, the Epsilon and Gammaproteobacteria. These analyses, however, were based on samples collected from a single body region, the setae of pereopods. To more thoroughly investigate the microbiome associated with *Kiwa puravida*, a yeti crab species from Costa Rica, we utilized barcoded 16S rRNA amplicon pyrosequencing, as well as microscopy and terminal restriction fragment length polymorphism analysis. Results indicate that, indeed, the bacterial community on the pereopods is far less diverse than on the rest of the body (Shannon indices ranged from 1.30–2.02 and 2.22–2.66, respectively). Similarly, the bacterial communities associated with juveniles and adults were more complex than previously recognized, with as many as 46 bacterial families represented. Ontogenetic differences in the microbial community, from egg to juvenile to adult, included a dramatic under-representation of the Helicobacteraceae and higher abundances of both Thiotrichaceae and Methylococcaceae for the eggs, which paralleled patterns observed in another bacteria–crustacean symbiosis. The degree to which abiotic and biotic feedbacks influence the bacterial community on the crabs is still not known, but predictions suggest that both the local environment and host-derived factors influence the establishment and maintenance of microbes associated with the surfaces of aquatic animals.

Keywords: crab, deep-sea, epibiont, Kiwa, symbiosis

Received 9 May 2013; revision received 29 June 2013; accepted 2 July 2013

Introduction

Animals and plants are in continuous contact with microbes in the environment. In many cases, these microbes have become evolutionarily stable companions that positively influence the development, overall health and fitness of the host. For vertebrates in particular, for which we have learned a great deal due to the recent progress made by the Human Microbiome Project, there are unique microbial communities, some transient but most permanent, on different body regions from the digestive to the integumentary systems (Gill *et al*. 2006; Grice & Segre 2012; Human Microbiome Project Consortium 2012a,b; and many others). Most invertebrates have also been found to possess resident internal and external microbiomes, with similarly profound impacts on overall host health and survival. For example, fruit flies benefit from microbiome modulation of their developmental rate (Shin *et al*. 2011), sponges have an impressive chemical repertoire that is now confidently attributed to their diverse microbiome (Hentschel *et al*. 2012), and at least 20 phytophagous insect families derive nutritional and protective benefits from enduring associations with microbes (Wernegreen 2002; Dillon & Dillon 2004; Douglas 2009).

Correspondence: Shana K. Goffredi, Fax: +1 (323) 341-4974; E-mail: sgoffredi@oxy.edu

Combined molecular and ecological studies on microbial communities associated with the surfaces of animals have shown that prevailing physical and chemical conditions, such as temperature, pH, oxygen, moisture content and nutrients, greatly affect microbial community structure (Dethlefsen *et al.* 2007; Dewhirst *et al.* 2010). Spatial heterogeneity, even at mm-cm scales, can influence bacterial status on animal surfaces. The complex microbial ecosystem associated with the human body is one of the best examples of this phenomenon, with oily sebaceous areas hosting less diversity dominated by a few species and dry body regions possessing much higher diversity (Grice *et al.* 2009). Similarly, the microbial communities affiliated with animals, and plants, are dynamic over time. For mammalian gastrointestinal tracts, for example, bacterial community structure depends greatly upon the age of the individuals, from infancy to ageing adults, with, for example, the early human microbiome dominated by Firmicutes and the adult community dominated by Bacteroidetes (Biagi *et al.* 2010; Claesson *et al.* 2011; Koenig *et al.* 2011; Li *et al.* 2012).

The outer body surfaces of aquatic animals, in particular, represent highly dynamic and accessible interfaces for microbial growth. In some cases, these relationships appear to be persistent as adult hosts, including crustaceans, nematodes, polychaetes and gastropods, are never observed to be free of epibiotic bacteria (Van Dover *et al.* 1988; Polz *et al.* 1992; Haddad *et al.* 1995; Goffredi *et al.* 2004). Some of these episymbioses confer protection or defence from predators or the environment itself, some are nutritional in nature, and many still are of unknown function. The specific mechanisms for recognition and attachment between partners, and the modes of transmission between host generations have been either shown or suggested for a few of these associations (Nussbaumer *et al.* 2004; Bulgheresi *et al.* 2006; Dattagupta *et al.* 2009). Less is known, however, about the variability among bacterial inhabitants on aquatic invertebrates across body regions and across life stages. For example, a high degree of spatial heterogeneity in *Montastraea* coral-associated bacteria, at different locations only centimetres apart, was found across individual colonies and was suggested to explain the unpredictable initiation of coral disease symptoms at various locations on the host surface (Daniels *et al.* 2011). Similarly, a temporal sequence of microbial establishment in *Hydra* has been observed, with high microbial diversity in the 1st week after hatching, followed by an eventual progressive evolution of the less-diverse stable adult community (Franzenburg *et al.* 2013).

The purpose of the present study was to examine, via microbial taxonomic profiling of the 16S rRNA gene, patterns in the bacterial community structure associated with the cold-seep yeti crab, *Kiwa puravida*, from the Costa Rica margin (Thurber *et al.* 2011). Crabs within the family Kiwaidae, first described from hydrothermal vents along the Pacific-Antarctic Ridge (Macpherson *et al.* 2005) and most recently along the East Scotia Ridge (Rogers *et al.* 2012), are known to possess specialized setae colonized by numerous filamentous bacteria, giving them an unusually hairy appearance. Other crustaceans, including those from hydrothermal vents and freshwater caves, have also been found to associate with very similar bacteria, primarily within the Helicobacteraceae and Thiotrichaceae (Zbinden *et al.* 2008; Dattagupta *et al.* 2009; Petersen *et al.* 2009), suggesting that these particular bacteria preferentially form ectosymbioses with aquatic crustaceans (Goffredi 2010). In all cases, except one, only the specialized setae have been examined for bacterial presence on 'hairy' crustaceans; thus, the question remains whether spatial heterogeneity among body sites influences bacterial diversity. A recent study examining microbial communities on the hydrothermal vent shrimp *Rimicaris exoculata* revealed ontogenetic changes in the dominant proteobacteria between early and later life cycle stages (Guri *et al.* 2012); however, these authors suggested that 'deeper' sequencing would be valuable towards accurately elucidating bacterial diversity, as they, and others, have been limited by clone libraries yielding fewer than approximately 100 ribotypes per sample (Goffredi *et al.* 2008; Petersen *et al.* 2009; Hügler *et al.* 2011; Thurber *et al.* 2011; Tsuchida *et al.* 2011). The current study provides the first examination of epibiotic populations associated with aquatic crustaceans, from egg to juvenile to adult life stages and among adult body regions, using barcoded 16S rRNA amplicon pyrosequencing, complemented by terminal restriction fragment length polymorphism analysis, fluorescence *in situ* hybridization and transmission electron microscopy.

Materials and methods

Sample collection

Specimens of *Kiwa puravida*, including eggs, juveniles (approximately 2–9 mm postorbital carapace length) and adults (>22 mm length), were collected with *D.S.R.V.* Alvin on *R.V.* Atlantis expeditions AT15-44 and AT15-59 (22 Feb and 5 Mar 2009 and 7–10 Jan 2010, respectively) at Mound 12 offshore southwest Costa Rica (8°55.89N/84°18.89W) at depths of 1000–1040 m (Table 1; Figs 1, S1, Supporting information). Mound 12 is one of the several mud mounds (30 m high, 600 m across) in the area with active methane venting and authigenic carbonate concretions, as a result of subduction erosion, faulting and microbial activity. This site has been described in more detail by Han *et al.* 2004).

Table 1 Specimens of *K. puravida* used in this study, including life stage, size, collection information and corresponding analytical methods

Cruise*	Dive†	Date	Life stage	Size‡(mm)	Designation	Analysis§
AT15-44	A4501	Feb 2009	Adult	25	A4501_A25	barcoded (EC)
			Adult	35	A4501_A35	barcoded (EC)
			Juvenile	2.5	A4501_J2.5	barcoded (EC)
	A4511	Mar 2009	Juvenile	2	A4511_J2	barcoded (EC)
			Juvenile	2.5	A4511_J2.5	barcoded (EC)
			Juvenile	3	A4511_J3	barcoded (EC/CL)
			Juvenile	3.5	A4511_J3.5	barcoded (EC)
			Juvenile	4	A4511_J4	FISH
			Juvenile	4.5	A4511_J4.5	barcoded (EC)
			Juvenile	6	A4511_J6	TEM
AT15-59	A4586	Jan 2010	Adult	22	A4586_A22	barcoded (CL)/tRFLP
			Juvenile	9	A4586_J9	barcoded (CL)
	A4587	Jan 2010	Eggs	1	A4587_Egg	barcoded (EC/CL)/tRFLP
	A4589	Jan 2010	Juvenile	1.5	A4589_J1.5	barcoded (EC)/tRFLP
			Juvenile	5	A4589_J5	barcoded (CL)

*Cruise numbers correspond to those of the *R.V. Atlantis.*
†Dive numbers begin with A for the manned deep submergence research vehicle *Alvin* (owned and operated by the Woods Hole Oceanographic Institute).
‡Postorbital carapace length.
§EC indicates samples barcoded using the 16S rRNA primers 515F/806R, while CL indicates samples barcoded using the 16S rRNA primers 9F/541R.

Immediately upon collection, specimens were surface-treated with 100% ethanol and either preserved in cold 70% ethanol and stored at 4 °C until processing, preserved in 3% sucrose-buffered paraformaldehyde for fluorescence *in situ* hybridization (FISH) microscopy or preserved in 3% sucrose-buffered glutaraldehyde for electron microscopy. The eggs were recovered from the abdomen of a brooding female from dive A4587. Juveniles and eggs were initially examined using a Leica S8APO stereomicroscope and photographed with a Nikon Coolpix P6000 digital camera (Figs 1, S1, Supporting information). Limitations of sampling the larger animals and sharing among all scientific parties interested in *Kiwa* resulted in our analysis of only one whole-body adult sample and eggs from only one female. We believe the patterns of bacterial diversity, at least at the family level, are representative for the *Kiwa puravida* population, as many are present in all life stages and are consistent among diverse crustaceans (see Discussion).

DNA extraction and host identity

The DNEASY kit (Qiagen, Valencia, CA, USA) was used to extract total DNA from each *Kiwa puravida* specimen or sample. In most cases, we digested the entire specimen; however, for the adult yeti crab, body regions were subdissected and extracted (Table 2). For the adult whole-body-normalized (WBN) sample, care was taken to avoid crab host tissue and DNA extracts from each region of the exoskeleton were normalized to 30 ng/μL and pooled. Host crab identity was confirmed by phylogenetic comparison with previously published 18S rRNA gene sequences, amplified using the primers 3F (5′-GTTCGATTC-CGGAGAGGGA-3′) and 5R (5′- CTTGGCAAATGCTTTCGC-3′) published previously (Giribet *et al.* 1996). Thermal cycling conditions included 60 s each of denaturation at 94 °C, annealing at 54 °C, elongation at 72 °C (25 cycles) and a final extension at 72 °C for 6 min. 18S rRNA sequences were compared, via BLASTN, with yeti crab sequences available in GenBank and with each other using Sequencher, version 4.10.1 (GeneCodes Corp.). All specimens, including the eggs, were shown to be >99% similar to other *Kiwa* species (*Kiwa hirsuta*, *K. puravida* and the species from the East Scotia Ridge) at the 18S rRNA gene level. Further, these *Kiwa* species were more than 99% similar to each other (via 18S rRNA) and only 89% similar to the next closest anomuran (Macpherson *et al.* 2005; Thurber *et al.* 2011; Rogers *et al.* 2012). The 18S rRNA gene sequence for the type specimen of *K. puravida* is DQ219316 (Thurber *et al.* 2011).

16S rRNA terminal restriction fragment length polymorphism

Terminal restriction fragment length polymorphism (T-RFLP) analysis of bacterial 16S rRNA genes was

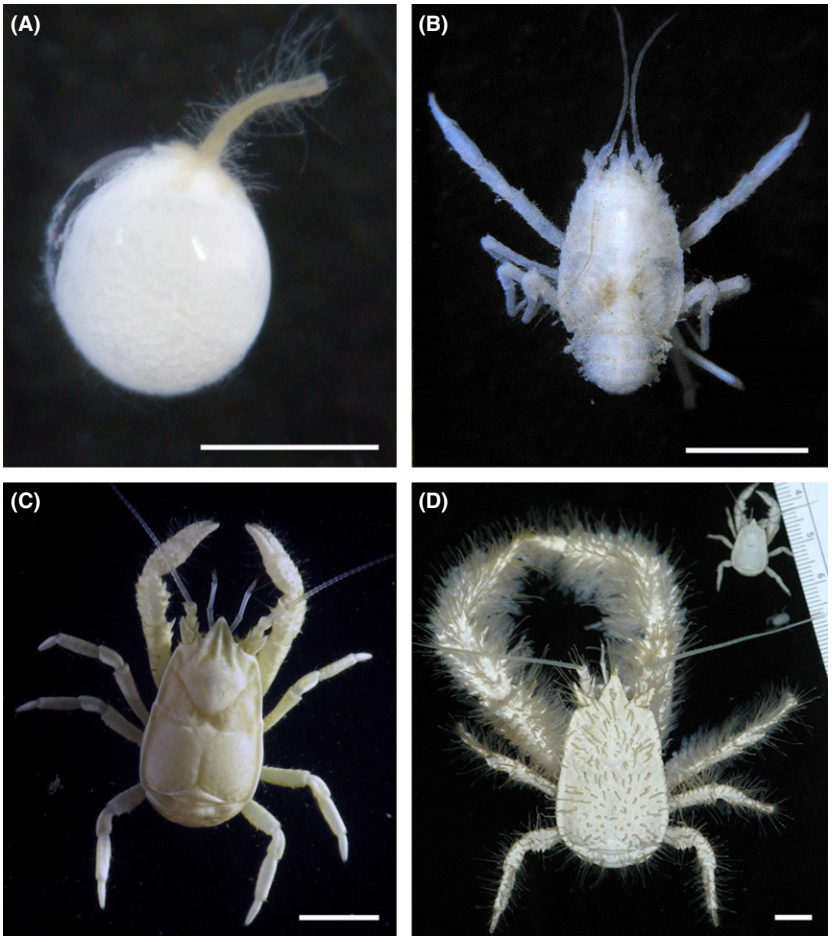

Fig. 1 *Kiwa puravida*. (A) Egg collected from a brooding adult female. Note the obvious filamentous bacteria attached. Scale, 1 mm. (B,C) Juvenile crabs. Scale, 1 mm. (D) Adult specimen, shown alongside a smaller juvenile, and ruler, at top right. Scale, 1 cm.

used to characterize the diversity and relative proportions of bacteria on 14 individual body regions (Table 2, S1, Supporting information). The 16S rRNA gene from purified DNA samples was PCR-amplified using bacterial primers 27F (fluorescently labelled with WellRED dye D4, Sigma-Proligo) and 1492R using PCR conditions described in the study of Goffredi *et al*. 2008 for unlabelled PCR. For each sample, duplicate PCR amplifications were normalized (300 ng) and pooled prior to digestion with *Hae*III (for 6–8 h at 37C; New England Biolabs). Digested products were precipitated using glycogen and sodium acetate as carriers and resuspended in 40 μL of formamide containing 0.5 μL of an internal dye standard (GenomeLab DNA size 600, labelled with WellRED dye D1; Beckman Coulter). Fluorescently labelled fragments were separated by capillary electrophoresis and analysed on a CEQ 8800 Genetic Analysis System (Beckman Coulter). Fragment sizes were parsed by separation of >3 bp, and relative abundances were estimated using the CEQ 8800 Fragment Analysis software. Diversity was assessed by the number of peaks obtained after restriction with *Hae*III and calculated using the Shannon–Wiener index (H′) according to the equation $H' = -\sum(pi)(\ln pi)$, where pi was the normalized area under each T-RFLP fragment peak within each sample (Table 2).

Barcoded 16S rRNA amplicon pyrosequencing

Bacterial 16S rRNA genes were PCR-amplified using a forward primer modified on the 5′ end to contain the 454 Life Sciences adapter B, a 2-bp linker sequence (GT), and the broadly conserved bacterial 515F primer (5′-GCCTTGCCAGCCCGCT-CAGGTGTGC CAGCMGCCGCGGTAA-3′), and a reverse primer modified on the 5′ end to contain the 454 Life Sciences adapter A, a 'GG'-bp linker sequence, and the bacterial primer 806R (5′-GCCTCCCTCGCGCCATCAG*X*GGGGACTACVSGGGT A-TCTAAT-3′). The reverse primers also contained a unique 7- to 12-bp barcode sequence (*X*) positioned between the primer sequence and the adapter to barcode each PCR product. Thermocycling conditions were as follows: 95 °C for 5 min; then 30 cycles of 95 °C for 30 s, 55 °C for 45 s, 72 °C for 90 s; and then 72 °C for 10 min. Each sample was amplified in triplicate, pooled and cleaned using the MoBio UltraClean 96-well PCR clean-up kit according to the manufacturer's

Table 2 Shannon–Wiener diversity index (H′) values, based on bacterial 16S rRNA terminal fragment length polymorphism profiles, from 14 different body regions of an adult *Kiwa puravida* from the Costa Rica margin

Yeti crab body region	Shannon H′*	Schematic of body regions‡ with H′ overlay
pereopod 1_mid†	1.301	
pereopod 1_distal	1.596	
carapace_lateral	1.744	
pereopod 1_proximal	1.815	
pereopod 4_proximal	1.816	
pereopod 3_proximal	2.019	
antennule_antennae	2.147	
whole-body-normalized	*2.168*	
dorsal carapace_mid	2.217	
dorsal carapace_anterior	2.349	
sternum_whole	2.362	
dorsal carapace_lower	2.417	
carapace_posterior_abdominal	2.499	
maxillae	2.634	
mandible-maxillae	2.655	

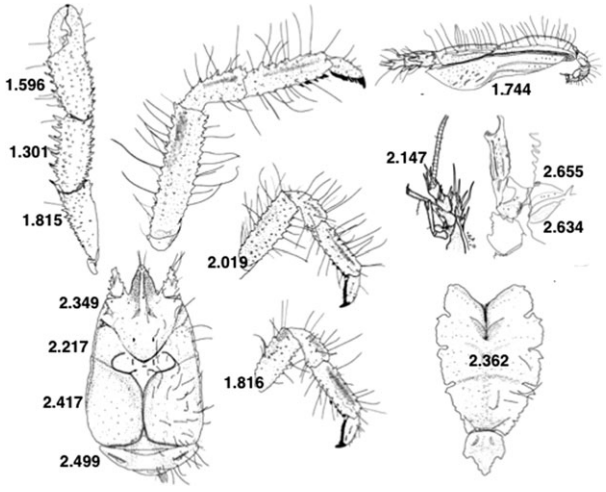

*Listed in order of ascending Shannon index based on tRFLP. Similar patterns for J′ and 1-λ′ were observed, except for carapace_lateral, which was lower than expected for 1-λ′.
†Pereopod 1 is the cheliped, and pereopods 2–5 are the walking legs.
‡Modified from Thurber *et al*. 2011.

instructions. The samples were sent to the Environmental Genomics Core Facility at the University of South Carolina for pyrosequencing on a Roche/454 Life Sciences Genome Sequencer FLX machine. Four samples were also selected for pyrosequencing at Chunlab Inc. (Seoul, Korea), also using a Roche/454 GS FLX Titanium platform. In this case, the 16S rRNA gene was amplified, as above, using the primers V1-9F (5′-CCTATCCCCTGTGTGCCTTGGCAGTC-ACGAGTTTGATC-MTGGCTCAG-3′) and V3-541R (5′CCATCTCATCCCTGCGTGTCTCCGAC*X*AC-WTTACCGCGGCTGCTGG-3′), where *X* indicates the unique barcode for each sample and the underline indicates the linker, followed by the primer. Between 839 and 4680 16S rRNA barcodes were generated per sample, exceeding what is estimated to be necessary to saturate diversity for similar samples (Guri *et al*. 2012; data not shown). We did not observe a correlation between sampling effort and diversity (slope = 0.0004, $R^2 = 0.18$, for the diversity metrics shown in Table 3). Additionally, to test for consistency between the sequencing facilities, two of the most diverse samples (eggs and juvenile A4511_J3) were analysed and compared. Results from both facilities were very similar in terms of measures of diversity and numbers of families recovered, despite different methods (Table S3, Supporting information). Resulting sequences were quality-filtered and dereplicated using the QIIME script split_libraries.py (Caporaso *et al*. 2010), checked for chimeras against the GreenGenes database using uchime, version 3.0.617 (Edgar *et al*. 2011), and subjected to the following procedures using QIIME scripts with the default settings: (i) sequences were clustered at 97% similarity; (ii) cluster representatives were selected; (iii) GreenGenes taxonomy was assigned to the cluster representatives using BLAST and (iv) tables with the abundance of different OTUs (and their taxonomic assignments) in each sample were generated. Due to an inability to make genus-level assumptions about taxonomy based on 200- to 500-bp 16S rRNA barcodes, we used conservative family-level designations to parse the data (Tables 4, S2, Supporting information). Nevertheless, a figure showing the common OTUs (>97% 16S rRNA distinction) and the relative abundance of each per sample is shown in Figure S2 (Supporting information). RStudio was used to make a heat map based on these family-level designations (Fig. 2), using a script available at https://github.com/Ecogenomics. Diversity estimates (Table 3), similarity percentages and principal component analysis plots (Figure S3, Supporting information) of pyrosequencing data were performed using Primer, version 6 (Clarke & Gorley 2006).

Electron microscopy

For examination by transmission (TEM) electron microscopy, samples (approximately 1 mm^3) were fixed in 3% glutaraldehyde buffered with 0.1 M phosphate and 0.3 M sucrose (pH 7.8). Following a wash in 0.1 M sodium cacodylate containing 24% sucrose, samples were postfixed with 1% OsO_4 in 0.1 M sodium cacodylate for 1 h, stained *en bloc* in 3% uranyl acetate in 0.1 M sodium acetate buffer for 1 h, dehydrated

Table 3 Bacterial community diversity estimations, based on 16S rRNA pyrosequencing analysis, for *Kiwa puravida* from the Costa Rica margin

Sample	Stage	Taxa*	Shannon DI (H′)	Evenness (J′)	Pielou's (1-λ′)
A4587_Egg	egg	49	2.615	0.672	0.854
A4589_J1.5	juv	41	1.596	0.430	0.572
A4511_J2	juv	26	1.307	0.401	0.556
A4501_J2.5	juv	37	2.016	0.558	0.761
A4511_J2.5	juv	28	1.480	0.444	0.628
A4511_J3	juv	31	1.785	0.520	0.742
A4511_J3.5	juv	24	1.341	0.422	0.592
A4511_J4.5	juv	13	1.264	0.493	0.635
A4589_J5	juv	34	1.417	0.402	0.604
A4586_J9	juv	39	1.306	0.357	0.578
A4586_A22	adult	46	1.353	0.353	0.531
A4501_A35_P	adult	21	1.061	0.348	0.540
A4501_A25_Pm†	adult	13	0.996	0.388	0.455
A4501_A25_Pd†	adult	17	1.155	0.408	0.545
A4501_A25_M‡	adult	21	1.427	0.469	0.625

*Taxa, in this case, were based on family-level designations.
†A4501 A25-Pd is a distal pereopod sample and A4501 A25-Pm is a mid-pereopod sample, both from adults A4501-A25.
‡A4501 A25-M is the mandible–maxillae samples from adult A4501-A25.

through an ethanol series, then infiltrated and embedded in Spurr's resin (Ted Pella, Redding, CA, USA). Thick (0.4 μm) and thin (70 nm) sections were stained with methylene blue and lead citrate, respectively, then examined and photographed using a Zeiss Labrolux 12 light microscope and Zeiss EM109 TEM (Figure 3). *Kiwa* specimens for SEM were fixed in 3% glutaraldehyde buffered with 0.1 M phosphate and 0.3 M sucrose (pH 7.8) and subsequently HMDS (hexamethyldisilazane)-dried, palladium-coated, and examined with an FEI Phenom instrument (Fig. 4B,D).

Fluorescence In situ hybridization microscopy

Yeti crabs, initially preserved in cold paraformaldehyde for 24 h, were rinsed twice with 1X phosphate-buffered saline (PBS), transferred to 70% ethanol and stored at −20 °C. Samples were embedded in Steedman's wax (one part cetyl alcohol was added to nine parts polyethylene glycol (400) distearate, mixed at 60 °C; Steedman 1957) and added to the sample in an ethanol/resin gradient of 3:1, 2:1 and 1:1, according to Pernthaler & Pernthaler (2005). Samples eventually embedded in full strength wax were allowed to solidify, sectioned (5–10 μm thick) using a Leica RM2125 manual microtome and placed onto Superfrost Plus slides (Fisher Scientific). Samples were dewaxed by three rinses in 100% ethanol (10 min each), followed by rehydration in 70% ethanol (10 min). Hybridization and wash buffers were made as described previously (Pernthaler & Pernthaler 2005), using 35% formamide in the hybridization buffer and 450 mM NaCl in the wash solution. A universal bacterial probe set (EUB338I-III, Amann *et al.* 1990; Daims *et al.* 1999), along with group-specific probes for Gammaproteobacteria (Gam42a; Manz *et al.* 1992) and Epsilonproteobacteria (EPS549; Lin *et al.* 2006), was labelled with either Cy3 or fluorescein. Hybridizations were typically 3–8 h, followed by washes of 15 min. Tissues were counter-stained with a dilute 4′6′-diamidino-2-phenylindole (DAPI) solution (5 mg mL-1) for 1 min and examined under epifluorescence microscope using a Nikon E80i epifluorescence research microscope with a Nikon DS-Qi1Mc high-sensitivity monochrome digital camera (Figs 4 A/C, 5 B–E and 6 A–K).

Results and discussion

Remarkably 'hairy' crustaceans in at least five families have been reported from both marine and freshwater environments (Zbinden *et al.* 2008; Dattagupta *et al.* 2009; Petersen *et al.* 2009; Suzuki *et al.* 2009; Tsuchida *et al.* 2011). The most recent addition to this motley crew was the now infamous 'yeti' crabs, within the family Kiwaidae (Macpherson *et al.* 2005), which, like the others, have a fuzzy white appearance resembling the mythological Himalayan creature. This decapod family was first described in 2004 after the discovery of *Kiwa hirsuta* from the Pacific-Antarctic Ridge (Macpherson *et al.* 2005). Since then, two additional species, *Kiwa puravida* from the Costa Rica margin (Thurber *et al.* 2011) and *Kiwa* n. sp. from the East Scotia Ridge (Rogers *et al.* 2012), have been discovered. All three species are known to have

Table 4 Summary of bacterial community structure, to the family level, based on 16S rRNA pyrosequencing analysis, for yeti crabs and eggs in this study, based on the Greengenes taxon assignments. Numbers shown indicate the percentage of the community

Taxon – Family level	egg	Juvenile avg (std)*	WBN adult	Closest relatives (uncultured habitat / cultured)‡
Epsilonproteobacteria				
Helicobacteraceae	3.1	54.8 (8.0)	66.4	*Rimicaris* / PAR *Kiwa* epibionts (99%) *Sulfurovum lithottrophicum* (93%)
Gammaproteobacteria				
Thiotrichaceae	32.5	17.3 (7.5)	15.2	*Shinkaia* / PAR *Kiwa* epibionts (99%) *Leucothrix mucor* (93%)
Methylococcaceae	24.3	2.2 (5.5)	5.7	*Rimicaris* epibionts (99%) *Methylomonas methanica* (95%)
Deltaproteobacteria				
Desulfobulbaceae	1.3	10.2 (7.1)	2.9	*Rimicaris* epibionts (99%) *Desulfocapsa sulfiexigens* (97%)
Bacteroidetes				
Flavobacteriaceae	4.3	4.8 (1.9)	1.6	*Rimicaris* epibionts (99%) *Polaribacter butkevichii* (93%)
Saprospiraceae	2.0	2.7 (2.0)	1.2	Hydrothermal vents (98%) *Lewinella marina* (89%)
Betaproteobacteria				
Comamonadaceae	3.0	0.0	0.0	Salt water lake (100%) *Acidovorax temperans* (99%)
Methylophilaceae	2.6	0.0	0.0	Coral associated (100%) *Aquabacterium commune* (99%)
Alphaproteobacteria				
Rhodobacteraceae	2.7	1.3 (0.2)	0.3	Arctic sediment (98%) *Leisingera aquamarina* (96%)
Verrucomicrobia				
Verrucomicrobiaceae	2.4	0.0	0.0	Hydrothermal vents (97%) *Rubritalea spongiae* (87%)
Others†				
< 1% for all samples	21.5	6.7	7.1	

*n = 8 juveniles, from 2–9mm length
†see Table S2 for more details
‡ the percentage shown in this column is the % similarity, based on 16S rRNA
PAR = Pacific Antarctic Ridge, WBN = whole body normalized

chelipeds and walking legs with setae that are densely colonized by numerous filamentous bacteria primarily within the Epsilon and Gammaproteobacteria (Goffredi *et al.* 2008; Goffredi 2010; Thurber *et al.* 2011). We describe here the comparative diversity of bacteria associated with various body regions of adult yeti crabs, as well as the bacterial community structure of eggs, juveniles (2–9 mm postorbital carapace length) and adults (>22 mm length). Results suggest variability in bacterial community structure and increased diversity in sites other than the pereopods. Additionally, ontogenetic changes in both bacterial dominance and diversity, from egg to juvenile to adult, were strikingly concordant with changes observed in the vent shrimp *Rimicaris exoculata* (Guri *et al.* 2012). Among juvenile yeti crabs, there were additional patterns in bacterial assemblage that may be related to host ecdysis and the geological setting from which they were collected.

General trends in bacterial community composition among body sites

The bacterial community varied among 14 body regions of an individual adult *Kiwa puravida*, with the lowest diversity observed for pereopods (Shannon indices of 1.30–2.02, depending on distance from the carapace) and a much higher diversity observed for all other carapace-associated regions and mouthparts (reflected in Shannon indices of 2.22–2.66; Table 2). The carapace region of crustaceans is historically known to host numerous bacteria at abundances up to 10^6 cm^{-2} (Becker 1996). Setae from mid-distal pereopods of *Kiwa*, with the lowest diversity in this study, have been the site of bacterial examination in previous studies (Goffredi *et al.* 2008; Goffredi 2010; Thurber *et al.* 2011), suggesting a significant underestimate of bacterial diversity associated with these crabs. The mouthparts, including maxillae and

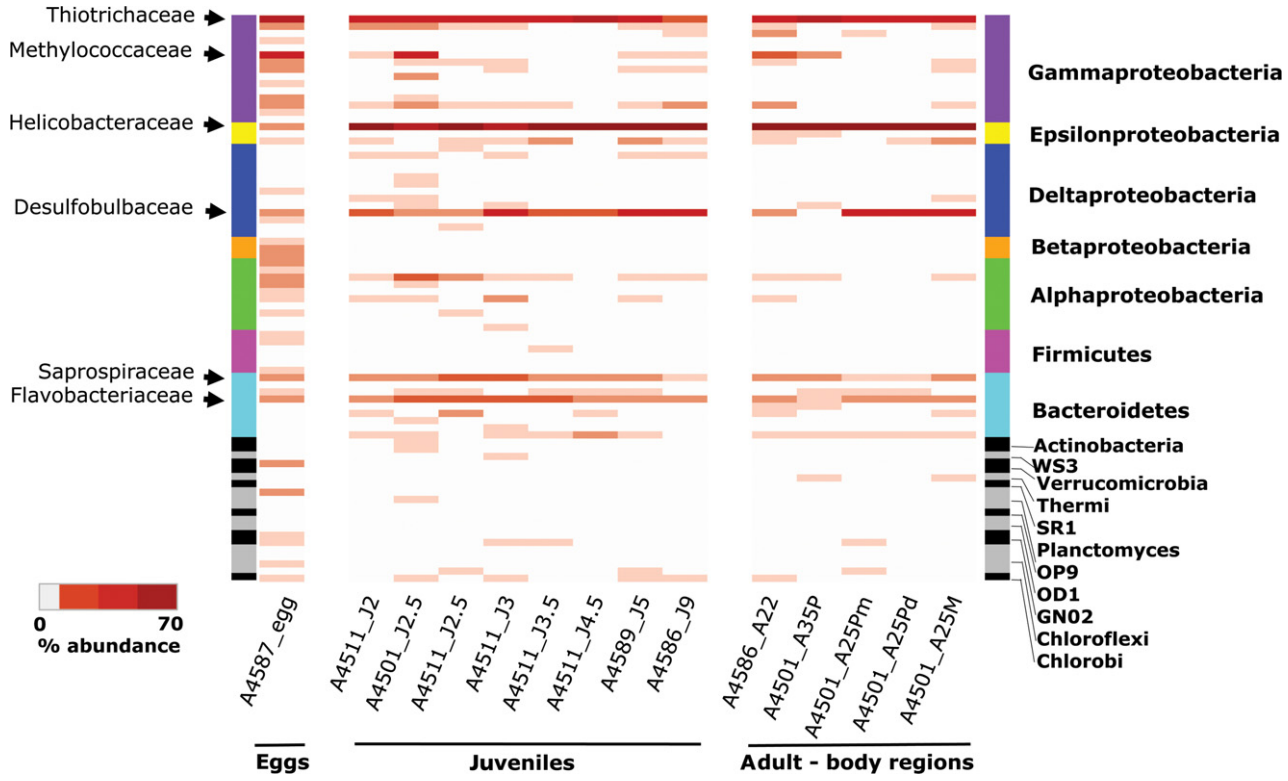

Fig. 2 Relative abundance of bacterial community structure, to the family level, based on 16S rRNA pyrosequencing analysis obtained from yeti crabs and eggs in this study. Each row represents a different bacterial family, and the abundance as a percentage of the total population is indicated by colour. A subset of family designations, based on GreenGenes assignment, is indicated on the left, while higher-level classifications (phylum and class) are indicated on the right. Colour scale indicates the abundance of each group, by percentage of the total community reads. Specimens are abbreviated as J for juvenile and A for adult, followed by the postorbital size, and whether the sample was from a specific body region (M = mouthparts, P = pereopod, d = distal, m = mid).

mandibles, had the highest bacterial diversity (2.66; Table 2). *Kiwa puravida* may periodically augment its diet through consumption of detritus, which was observed within the mouth of dissected individuals (Thurber *et al.* 2011). Transient detritus-associated bacteria may, therefore, be responsible for this higher measure of diversity. A pooled sample of DNA extracts, normalized to 30 ng/μL, for all 14 body regions (named 'whole-body-normalized') revealed a measured diversity estimate midway between the lowest and highest values, suggesting a more accurate representation of bacterial diversity for large adult yeti crabs (Tables 2, 3; Fig. 2). This whole-body-normalized (WBN) sample was used for subsequent barcoding analysis, in a comparison with earlier life stages (detailed in the next section) and body regions of other adults. Although, in general, barcoding analysis revealed much higher OTU numbers, similar trends in diversity were achieved with both tRFLP and barcoding analysis. For example, for both analyses, the mid-distal pereopod samples yielded the lowest Shannon diversity indices (approximately 1.3 and approximately 1.1, respectively, for tRFLP and barcode analysis), while the mouthparts and egg samples had the highest diversity (Shannon indices of approximately 2.6 for both tRFLP and barcode analysis).

Variation in bacteria across life stages of Kiwa individuals

Based on 16S rRNA pyrosequencing analysis, the bacterial community on both the adult and juvenile yeti crabs was more diverse than previously realized with members from up to 46 family-level groups represented (Tables 3, S2, Supporting information; Fig. 2). Bacterial communities on juveniles, in general, were more diverse than on the adult, with Shannon diversity indices of 1.26–2.02, as compared to 1.35 (Table 3). Sample discrimination analysis (SIMPER) suggested that the group of juveniles was 21% dissimilar from the whole-body-normalized adult and that slight differences (<10%) in Helicobacteraceae and Desulfobulbaceae, followed by Thiotrichaceae and Methylococcaceae, primarily drove the distinction between the two by cluster analysis. TEM and FISH microscopy confirmed a

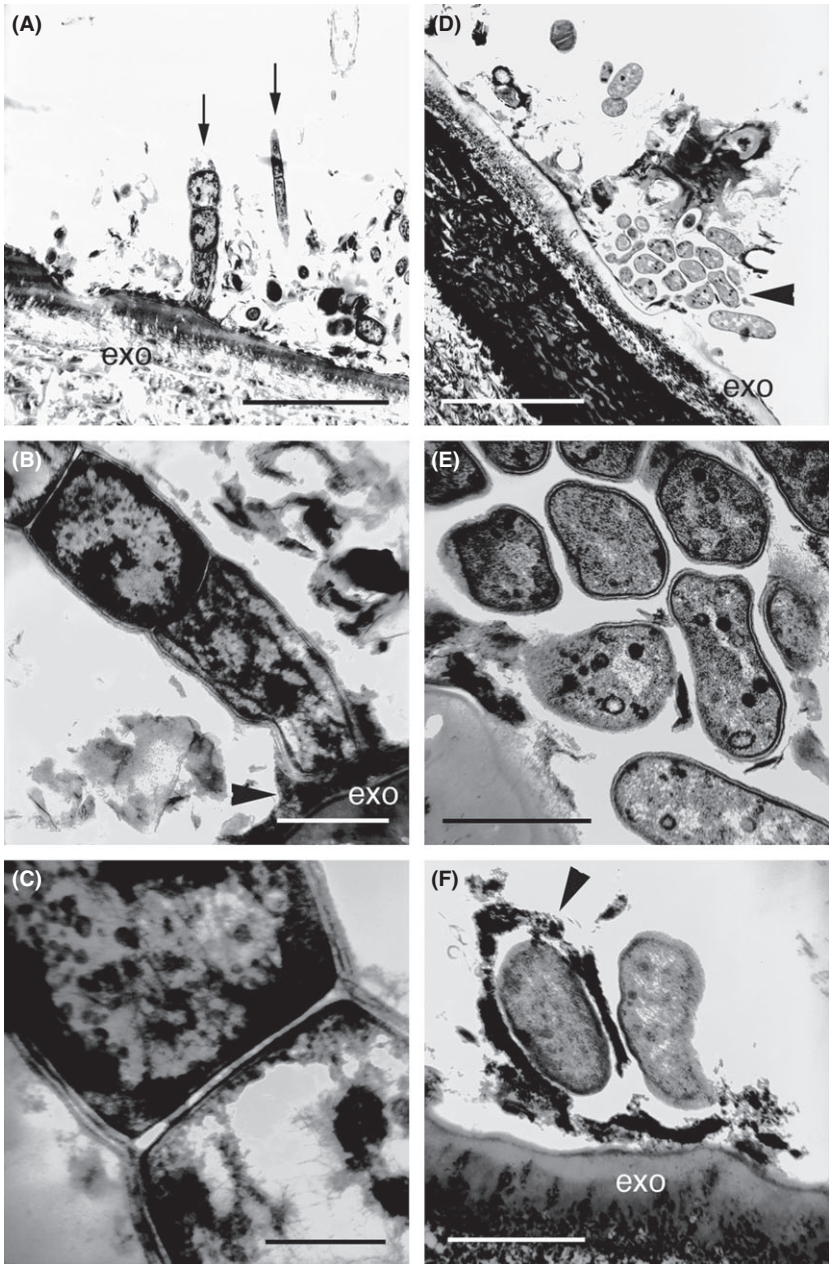

Fig. 3 Bacteria associated with a juvenile yeti crab, as shown by transmission electron microscopy. (A) Two filamentous morphotypes (arrows) associated with the exoskeleton (exo). Scale, 5 μm. (B) increased magnification showing the anchor-like structure at the base of the filament (arrowhead). Scale, 1 μm. (C) Increased magnification of B, showing the double membrane and cytoplasm. Scale, 0.5 μm. (D) A cluster of nonfilamentous morphotypes (arrowhead) associated with the exoskeleton (exo). Scale, 5 μm. (E) Increased magnification of D, showing the double membrane and cytoplasm of the cells. Scale, 1 μm. (F) Nonfilamentous bacteria attached to, and surrounded by, the exoskeleton (exo) by what appears to be an EPS (or exopolysaccharide-like material; arrowhead). Scale, 1 μm.

diverse bacterial community on juvenile crabs, based on numerous observable morphologies, including rods, cocci and various filamentous shapes (Figs 3–6). There was no direct positive correlation between juvenile size and diversity (Table 3, Fig. 2). Rather, juvenile A4511_J4.5, which was initially suspected of recent moulting (observable via stereomicroscopy; Fig. S1, Supporting information), had the lowest diversity of all whole animals analysed ($H' = 1.264$; Table 3). This particular juvenile, despite having the least-diverse microbial community among the juveniles analysed, was associated with all bacterial families found consistently in eggs through adults (Fig. 2), possibly suggesting the presence of a 'core' microbial community soon after ecdysis. The mechanism for continued maintenance of these ectosymbiotic associations, despite host ecdysis, is not known, yet microscopic observations of *Rimicaris exoculata* shrimps showed the formation of a new bacterial community within 2 days of moulting (Corbari *et al.* 2008).

Bacteria were observable on the juvenile yeti crabs via TEM and FISH microscopy (Figs 3–5), and as in other studies, the most conspicuous and dominant bacteria associated with the crabs were filamentous in nature (1–8 μm in diameter and of varying lengths). Consistent with previous studies on marine crustaceans,

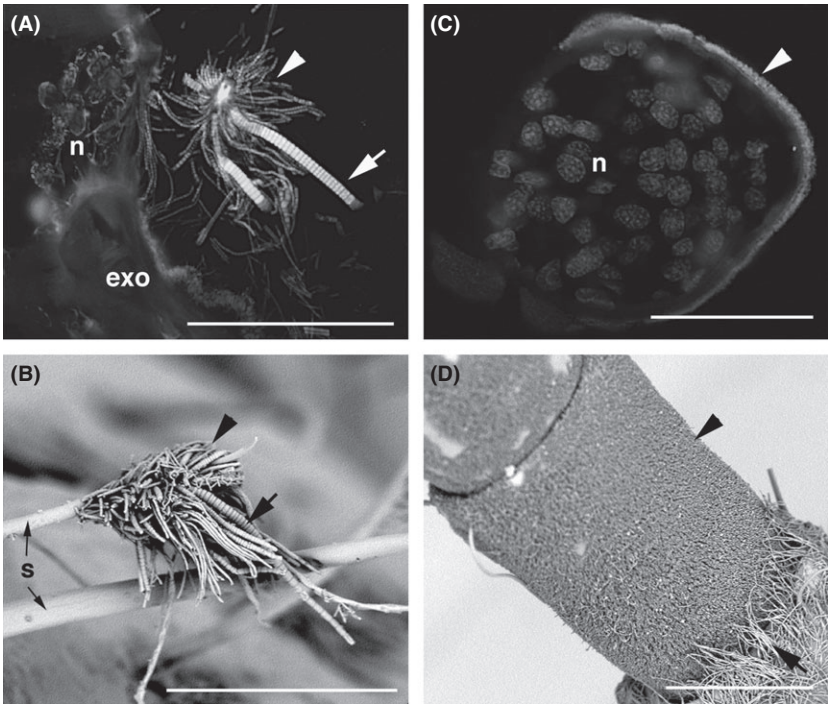

Fig. 4 Fluorescence *in situ* hybridization (FISH) microscopy and scanning electron microscopy (SEM) of bacteria associated with juvenile yeti crabs. (A) and (B) are FISH and SEM, respectively, of a setae covered in filamentous bacteria (near the mouthparts). At least two different morphotypes can be clearly observed (arrow and arrowhead). (C) and (D) are FISH and SEM, respectively, of an antennae primarily covered in nonfilamentous bacteria (arrowheads), as well as some filamentous types (arrow). The crab nuclei (n) were stained with DAPI. s = setae, exo = exoskeleton. All scale bars, 50 μm.

the thick filaments were identified as members of the Epsilonproteobacteria, while the thin filaments were Gammaproteobacteria (Fig. 6; Goffredi *et al.* 2008; Petersen *et al.* 2009; Ponsard *et al.* 2013). In addition to the dominant thin filaments, at least four other diverse Gammaproteobacterial morphotypes were observed by FISH microscopy (Fig. 6H–K). In previous studies, nonfilamentous morphotypes were rarely observed in association with the pereopod setae (Macpherson *et al.* 2005; Goffredi *et al.* 2008), yet when other body regions were examined in the present study, such as the antennae, abdomen and carapace, many other bacterial shapes were identified (Figs 4C–D, 6C,D, I,J; Goffredi 2010). Some bacteria appeared to be attached either via physical anchor points or via possible exopolysaccharide layers (Fig. 3B,F), as similarly described for epibionts found on *Rimicaris* (Corbari *et al.* 2008; Zbinden *et al.* 2008).

Despite the uncovered diversity of many minor groups, six core families comprised approximately 94% of the community diversity in both juveniles and adults, including members of the Epsilonproteobacteria, Gammaproteobacteria, Deltaproteobacteria and Bacteroidetes (Table 4, Fig. 2). As mentioned earlier, in past studies, *Kiwa* pereopod setae have been sampled exclusively and were dominated by the same major groups, primarily Helicobacteraceae (most closely related to *Sulvurovum* species) and Thiotrichaceae (most closely related to *Leucothrix* species, currently also designated *Cocleimonas* by the Ribosomal Database Project, although more distantly related; Tanaka *et al.* 2011). Relative abundances of Epsilon and Gammaproteobacteria associated with the crabs (57–72% and 10–32% of the community, respectively) were similar to values previously reported for both *Kiwa* species (50–82% and approximately 25%, respectively; Goffredi *et al.* 2008; Goffredi 2010). This variability in relative abundance suggests that the identity of the dominant proteobacterial players remains constant, but the composition changes, possibly depending upon biotic (body region, moulting) or abiotic (prevailing chemistry) conditions. As noted previously, these are the dominant, albeit variable, bacteria similarly found in association with other decapods, including *Rimicaris exoculata* and *Shinkaia crosnieri* (Table 4; Petersen *et al.* 2009; Tsuchida *et al.* 2011). This remarkably consistent microbial community, conserved not only among congeners of *Kiwa* from the Pacific Ocean (Goffredi *et al.* 2008; Thurber *et al.* 2011) and *Rimicaris* along the Mid Atlantic Ridge (Petersen *et al.* 2009; Guri *et al.* 2012), but even between crustacean families, further suggests a unique bacterial assemblage indigenous to the surfaces of marine invertebrates. Indeed, a comparison with 16S rRNA genes recovered from both rocks and sediments in the Mound 12 area revealed no matches at the 97% similarity cut-off (J. Marlow and A. Dekas, personal communication). Additional Gammaproteobacteria present on the yeti crabs included Methylococcaceae, Piscirickettsiaceae (some related to *Methylophaga*), and undefined Cardiobacteriales and Chromatiales (Table S2, Supporting information), supporting the diverse Gammaproteobac-

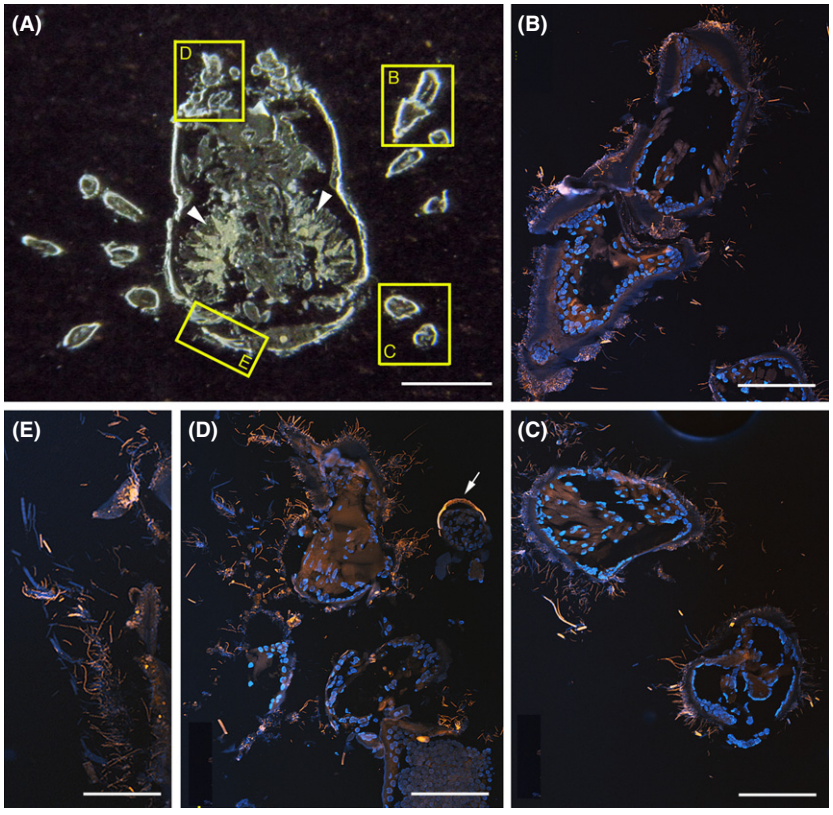

Fig. 5 Fluorescence *in situ* hybridization (FISH) microscopy of the bacteria associated with a juvenile yeti crab. (A) Cross-section through an entire juvenile yeti crab embedded in Steedman's wax. Boxes designate body regions in respective panels, including: (B), 1st pereopod (cheliped); (C), 4th walking leg; (D), base of the antennae; and (E), posterior abdominal carapace. Scale, 1 mm. (B–E) All bacteria are shown in orange (Eub338). The crab nuclei are shown in blue (stained with DAPI). The arrowheads in panel A show the gills. The arrow in panel D shows the antennae shown in Figure 4B. Scales, 100 μm.

terial morphotypes observed by FISH microscopy (Fig. 6H–K) and possibly in other studies on similarly setose crabs (Watsuji *et al.* 2010).

Bacteria associated with the juvenile yeti crabs were specifically different from the adult in community membership of the Desulfobulbaceae, closely related to *Desulfocapsa sulfexigens* (1–22% of the bacterial community), the Flavobacteriaceae and Saprospiraceae (2–7% and 1–6%, respectively), and the presence of Methylococcaceae, most closely related to *Methylomonas methanica* (0–16% of the community; Table 4, S2). The Desulfobulbaceae and Bacteroidetes have been observed previously, as minor yet consistent members on *Kiwa*, *Shinkaia* and *Rimicaris* individuals (Goffredi *et al.* 2008; Goffredi 2010; Hügler *et al.* 2011; Tsuchida *et al.* 2011). The Methylococcaceae are particularly interesting in that they have been observed previously on individuals of both *Shinkaia* and *Rimicaris* (Watsuji *et al.* 2010; Guri *et al.* 2012), yet in our study, the presence of these type I methanotrophs was highly variable, comprising approximately 6% of the bacterial community in the adult, 16% in a single juvenile (A4501_J2.5) and <1% in the other seven juveniles (Tables 4, S2, Supporting information). Sample discrimination analysis suggested that juvenile A4501_J2.5 was distinct from the rest (36% average dissimilarity) due to differences primarily in Methylococcaceae and Helicobacteraceae. For juvenile A4501_J2.5, the dominant Methylococcaceae were related to *Methylosarcina* (63% of the Methylococcaceae), *Methylomonas* (22%) and *Methylobacter* (14%). Juvenile A4501_J2.5 was the only specimen examined from a specific carbonate rock in an area of active methane venting. This observation, combined with a previous correlation between methanotroph epibiont abundance and high concentrations of methane in hydrothermal fluids (Watsuji *et al.* 2010), suggests that the environment may be partly responsible for the bacterial community structure on crustacean surfaces. Whether or not these bacteria represent a true 'episymbioses' between methanotrophic bacteria and the crab host, as suggested by Guri *et al.* (2012), is not known; however, compelling evidence exists for assimilation of ^{13}C-labelled methane into both the epibionts and muscle tissue of the *Shinkaia* crab from hydrothermal vents in the Okinawa Trough, Japan (Watsuji *et al.* 2010).

Eggs collected from a brooding female *Kiwa puravida* had the highest bacterial diversity of any sample or life stage, with a Shannon diversity value of 2.62 (Table 3). Principal component analysis affirmed the very different nature of the overall community structure associated with the eggs, compared with later life stages (Figure S3, Supporting information). The six dominant bacterial families comprised only 70% of the community on the eggs, whereas they were approximately 94% of

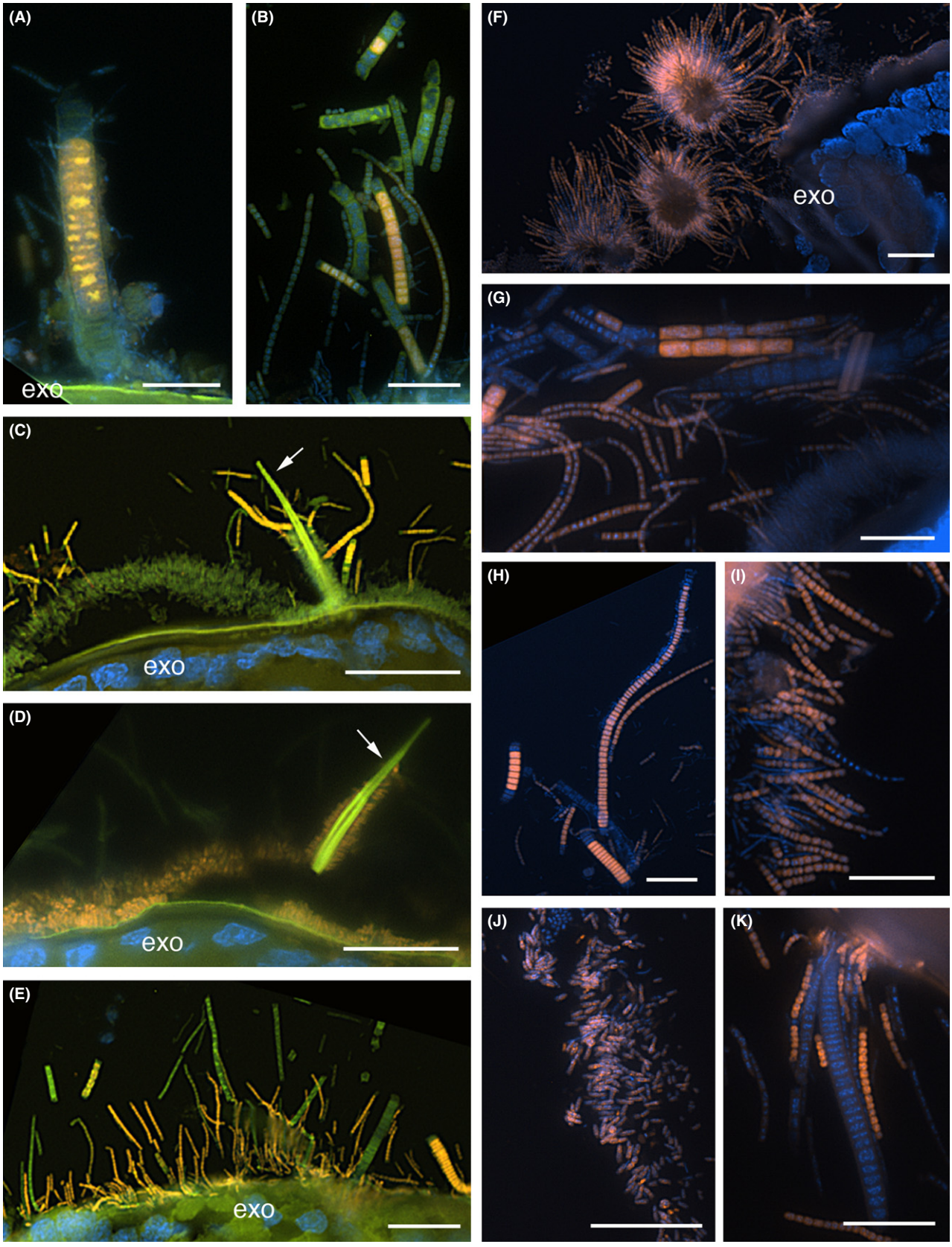

Fig. 6 Fluorescence *in situ* hybridization (FISH) microscopy of the bacteria associated with the juvenile yeti crab, shown in Figure 5A. (A,B) Epsilonproteobacteria, shown in orange (Cy3-EP549), with other bacteria shown in green (FITC-Eub338) or blue (DAPI). (C,D) A cross-section through the exoskeleton and setae, showing Epsilonproteobacteria in orange (panel C; EP549) and Gammproteobacteria in orange (panel D; Gam42). E. Gammaproteobacteria, shown in orange (Cy3-Gam42), with other bacteria shown in green (FITC-Eub338F). F. All bacteria (shown as orange; Cy3-Eub338) observed as tufts at the tops of setae. G. Epsilonproteobacteria, shown in orange (Cy3-EP549), with other bacteria shown in blue (DAPI). H-K. Four different morphotypes of associated Gammaproteobacteria, shown in orange (Cy3-Gam42), with other bacteria shown in blue (DAPI). In all cases, the crab nuclei are also shown in blue (stained with DAPI). exo = exoskeleton, arrow = setae. Body regions in respective panels include the 1st pereopod-mid (A, I), 1st pereopod tip (J), 2nd walking leg (F), 3rd walking leg (H), anterior carapace near base of antennae (B,C and D), posterior carapace (G), abdominal carapace (K) and the mouthparts (E). All scale bars, 10 μm.

the juvenile- and adult-associated communities (Table 4, S2, Supporting information). Sample discrimination analysis (SIMPER) suggested that the egg bacterial community was 68% dissimilar from the juveniles and whole-body-normalized adult. Notable differences between these dominant groups observed for eggs included a dramatic under-representation of the Helicobacteriaceae (only 3% of the bacterial community, compared to approximately 55–60%) and higher abundances of both Thiotrichaceae (approximately 33%, compared to 15–18%) and Methylococcaceae (24%, compared to 0–5%; Table 4; Figure S2, Supporting information). Other bacterial groups represented in the egg sample included 2–3% Comamonadaceae, Methylophilaceae, Verrucomicrobiaceae and undescribed members of Chromatiales, among many others at <1% of the community (Table S2, Supporting information). The differences in bacterial community composition between early and later life cycle stages in *Kiwa puravida* were strikingly similar to those observed for *Rimicaris exoculata* (Guri *et al*. 2012). Like *Kiwa*, molecular and microscopic analysis indicated that *R. exoculata* eggs were dominated by Gammaproteobacteria, whereas later stages were dominated by Epsilonproteobacteria (Guri *et al*. 2012). Whether this convergent ontogenetic change in dominant bacteria is related to factors inherent among the different bacterial types or the physical and chemical changes from egg to hatchling is not yet known. Similarly, Methylococcaceae were also most prominent on the eggs of *R. exoculata* (Guri *et al*. 2012). The affinity of these type I methanotrophic bacteria to the eggs of crustaceans may be explained by their use of methanol or methylamines, possibly emitted by the mucous-rich, ammonia-producing egg itself. Our data imply that most of the later-stage bacterial community members were present on the *Kiwa puravida* eggs, albeit at different levels (Figs 2, S2, Supporting information; Tables 4, S2, Supporting information), suggesting a complex interaction between inheritance and environmental exposure. Maternal transmission of epibionts during egg brooding is possible and has been suggested for the freshwater amphipod *Niphargus* (Dattagupta *et al*. 2009). We suspect that initial exposure to bacteria occurs in the brood chamber and is possibly shaped and winnowed, by environmental factors, to the community observed in the older juveniles and adults.

Conclusion

Yeti crabs, and other marine crustaceans, are colonized by complex bacterial communities, comprised of as many as 46 bacterial families with varying degrees of adaptation to life on animal surfaces. The processes controlling community membership are still poorly understood. For example, variability in bacterial composition may result for body regions that are disturbed more frequently by the host (e.g. grooming), or by a combination of physical, chemical and biological factors. Regardless, it does suggest that a single-point sample may not be representative of the total bacterial community associated with any particular host. In the case of *Kiwa puravida*, these surfaces appear to be more than just undefended areas grown over by bacteria, but rather are carefully controlled by the host. For example, *K. puravida* rhythmically waves its arm in seeping reduced fluids (Thurber *et al*. 2011), presumably to increase symbiont access to both oxygen and sulphide, which do not usually exist in the same water mass due to rapid chemical oxidation. Host control over the bacterial population implies that there must be some ecological value to the host. This value for many 'hairy' crustaceans is thought to be nutritional based on lipid and isotope data, modified morphology, behavioural observations and measures of fixed carbon incorporation by both partners (Miyake *et al*. 2007; Watsuji *et al*. 2010; Thurber *et al*. 2011).

In the present study, we also observed a significant difference in the bacterial community associated with eggs, as compared to young juveniles and the adult. The presence, however, of most juvenile/adult-stage bacterial members on the *Kiwa* eggs suggests a possible propagation of the symbiosis via direct contact with the maternal parent. Two ontogenetic patterns were strikingly consistent with those previously observed for other symbioses. The succession of a community dominated by Gammaproteobacteria (eggs) to one dominated by Epsilonproteobacteria (juveniles/adults) was similarly observed for the hydrothermal vent shrimp *Rimic-*

aris exoculata (Guri *et al.* 2012). The additional predominance of Methylococcaceae on the eggs of both *Kiwa* and *Rimicaris* is surprising and implies a possible affinity of these particular bacteria to crustacean eggs. Additionally, the increased bacterial diversity observed in community profiles for both *Kiwa* eggs and juveniles, as compared to the adult, is similar to that observed for *Hydra* (Franzenburg *et al.* 2013). Parallels to the formation of mammalian gut communities were drawn by Franzenburg and colleagues, including a prediction that both the local environment and host-derived factors influence the establishment of animal–microbial ecosystems, such as those associated with aquatic crustaceans.

Acknowledgements

The authors thank the *D.S.R.V. Alvin* pilots and *R.V. Atlantis* crew, chief scientists L. Levin (Scripps Institute of Oceanography) and V.J. Orphan (California Institute of Technology) for participation in the Costa Rica research cruises AT15-44 and AT15-59 in 2009 and 2010, respectively; A. Thurber (Oregon State University) for shipboard collaboration and information about *Kiwa puravida*; N. Fierer and D. Berg-Lyons (University of Colorado Boulder) for graciously processing the yeti samples for barcode analysis at Engencore; A. Skarshewski, M. Imelfort and M.F. Haroon (Australian Centre for Ecogenomics, University of Queensland) for bioinformatic assistance; G. Rouse (Scripps Institution of Oceanography) for photography (Fig. 1C); and Ms. L. Martin and Dr. G. Martin (Occidental College) for TEM images. Funding for undergraduate students was provided by an HHMI grant to Occidental College and the Undergraduate Research Center (Academic Student Projects) at Occidental College. We also thank three anonymous reviewers and Dr. S. Dattagupta, all of whom greatly improved the manuscript.

References

Amann RI, Binder BJ, Olson RJ, Chisholm SW, Devereux R, Stahl DA (1990) Combination of 16S rRNA-targeted oligonucleotide probes with flow cytometry for analyzing mixed microbial populations. *Applied and Environment Microbiology*, **56**, 1919–1925.

Becker K (1996) Epibionts on carapaces of some malacostracans from the Gulf of Thailand. *Journal of Crustacean Biology*, **16**, 92–104.

Biagi E, Nylund L, Candela M *et al.* (2010) Through ageing, and beyond: gut micro- biota and inflammatory status in seniors and centenarians. *PLoS ONE*, **5**, e10667.

Bulgheresi S, Schabussova I, Chen T, Mullin NP, Maizels RM, Ott JA. (2006) A new C-type lectin similar to the human immunoreceptor DC-SIGN mediates symbiont acquisition by a marine nematode. *Applied and Environmental Microbiology*, **72**, 2950–2956.

Caporaso JG, Kuczynski J, Stombaugh J *et al.* (2010) QIIME allows analysis of high-throughput community sequencing data. *Nature Methods*, **7**, 335–336.

Claesson MJ, Cusack S, O'Sullivan O *et al.* (2011) Composition, variability, and temporal stability of the intestinal microbiota of the elderly. *Proceedings of the National Academy of Sciences of the United States of America*, **108**, 4586–4591.

Clarke KR, Gorley RN (2006) PRIMER v6: User Manual/Tutorial PRIMER-E Plymouth.

Corbari L, Zbinden M, Cambon-Bonavita MA, Gaill F, Compere P (2008) Bacterial symbionts and mineral deposits in the branchial chamber of the hydrothermal vent shrimp *Rimicaris exoculata*: relationship to moult cycle. *Aquatic Biology*, **1**, 225–238.

Daims H, Brühl A, Amann R, Schleifer K-H, Wagner M (1999) The domain-specific probe EUB338 is insufficient for the detection of all Bacteria: development and evaluation of a more comprehensive probe set. *Systematic and Applied Microbiology*, **22**, 434–444.

Daniels CA, Zeifman A, Heym K *et al.* (2011) Spatial heterogeneity of bacterial communities in the mucus of *Montastraea annularis*. *Marine Ecology Progress Series*, **426**, 29–40.

Dattagupta S, Schaperdoth I, Montanari A *et al.* (2009) A novel symbiosis between chemoautotrophic bacteria and a freshwater cave amphipod. *The ISME Journal*, **3**, 935–943.

Dethlefsen L, McFall-Ngai M, Relman DA (2007) An ecological and evolutionary perspective on human-microbe mutualism and disease. *Nature*, **449**, 811–818.

Dewhirst FE, Chen T, Izard J *et al.* (2010) The human oral microbiome. *Journal of Bacteriology*, **192**, 5002–5017.

Dillon RJ, Dillon VM (2004) The gut bacteria of insects: nonpathogenic interactions. *Annual Review of Entomology*, **49**, 71–92.

Douglas AE (2009) The microbial dimension in insect nutritional ecology. *Functional Ecology*, **23**, 38–47.

Edgar RC, Haas BJ, Clemente JC, Quince C, Knight R (2011) UCHIME improves sensitivity and speed of chimera detection. *Bioinformatics*, **27**, 2194–2200.

Franzenburg S, Fraune S, Altrock PM *et al.* (2013) Bacterial colonization of *Hydra* hatchlings follows a robust temporal pattern. *The ISME Journal*, **7**, 781–790.

Gill SR, Pop M, Deboy RT *et al.* (2006) Metagenomic analysis of the human distal gut microbiome. *Science*, **312**, 1355–1359.

Giribet G, Carranza S, Baguñà J, Riutort M, Ribera C (1996) First molecular evidence for the existence of a Tardigrada + Arthropoda clade. *Molecular Biology and Evolution*, **13**, 76–84.

Goffredi SK (2010) Indigenous ectosymbiotic bacteria associated with diverse hydrothermal vent invertebrates. *Environmental Microbiology Reports*, **2**, 479–488.

Goffredi SK, Waren A, Orphan VJ, Van Dover CL, Vrijenhoek RC (2004) Novel forms of structural integration between microbes and a hydrothermal vent gastropod from the Indian Ocean. *Applied and Environment Microbiology*, **70**, 3082–3090.

Goffredi SK, Jones WJ, Erhlich H, Springer A, Vrijenhoek RC (2008) Epibiotic bacteria associated with the recently discovered Yeti crab, *Kiwa hirsuta*. *Environmental Microbiology*, **10**, 2623–2634.

Grice EA, Segre JA (2012) The human microbiome: our second genome. *Annual Review of Genomics and Human Genetics*, **13**, 151–170.

Grice EA, Kong HH, Conlan S *et al.* (2009) NISC Comparative Sequencing Program Topographical and temporal diversity of the human skin microbiome. *Science*, **324**, 1190–1192.

Guri M, Durand L, Cueff-Gauchard V *et al.* (2012) Acquisition of epibiotic bacteria along the life cycle of the hydrothermal shrimp *Rimicaris exoculata*. *The ISME Journal*, **6**, 597–609.

Haddad A, Camacho F, Durand P, Cary SC (1995) Phylogenetic characterization of the epibiotic bacteria associated with the hydrothermal vent polychaete *Alvinella pompejana*. *Applied and Environment Microbiology*, **61**, 1679–1687.

Han X, Suess E, Sahling H, Wallmann K (2004) Fluid venting activity on the Costa Rica Margin: new results from authigenic carbonates. *Geologische Rundschau*, **93**, 596–611.

Hentschel U, Piel J, Degnan SM, Taylor MW (2012) Genomic insights into the marine sponge microbiome. *Nature Reviews Microbiology*, **10**, 641–654.

Hügler M, Petersen JM, Dubilier N, Imhoff JF, Sievert SM (2011) Pathways of carbon and energy metabolism of the epibiotic community associated with the deep-sea hydrothermal vent shrimp *Rimicaris exoculata*. *PLoS Biology*, **6**, e16018.

Human Microbiome Project Consortium (2012a) A framework for human microbiome research. *Nature*, **486**, 215–221.

Human Microbiome Project Consortium (2012b) Structure, function and diversity of the healthy human microbiome. *Nature*, **486**, 207–214.

Koenig JE, Spor A, Scalfone N *et al.* (2011) Succession of microbial consortia in the developing infant gut microbiome. *Proceedings of the National Academy of Sciences of the United States of America*, **108**, 4578–4585.

Li RW, Connor EE, Li C, Baldwin Vi RL, Sparks ME (2012) Characterization of the rumen microbiota of pre-ruminant calves using metagenomic tools. *Environmental Microbiology*, **14**, 129–139.

Lin X, Wakeham SG, Putnam IF *et al.* (2006) Comparison of vertical distributions of prokaryotic assemblages in the anoxic Cariaco Basin and Black Sea by use of fluorescence *in situ* hybridization. *Applied Environmental Microbiology*, **72**, 2679–2690.

Macpherson E, Jones W, Segonzac M (2005) A new squat lobster family of *Galatheoidea* (*Crustacea*, *Decapoda*, *Anomura*) from the hydrothermal vents of the Pacific-Antarctic Ridge. *Zoosystema*, **27**, 709–723.

Manz W, Amann R, Ludwig W, Wagner M, Schleifer K-H (1992) Phylogenetic oligodeoxynucleotide probes for the major subclasses of *Proteobacteria*: problems and solutions. *Systematic Applied Microbiology*, **15**, 593–600.

Miyake H, Kitada M, Tsuchida S, Okuyama Y, Nakamura K (2007) Ecological aspects of hydrothermal vent animals in captivity at atmospheric pressure. *Marine Ecology*, **28**, 86–92.

Nussbaumer AD, Bright M, Baranyi C, Beisser CJ, Ott JA (2004) Attachment mechanism in a highly specific association between ectosymbiotic bacteria and marine nematodes. *Aquatic Microbial Ecology*, **34**, 239–246.

Pernthaler A, Pernthaler J (2005) Simultaneous fluorescence *in situ* hybridization of mRNA and rRNA for the detection of gene expression in environmental microbes. *Methods Enzymology*, **397**, 352–371.

Petersen JM, Ramette A, Lott C, Cambon-Bonavita MA, Zbinden M, Dubilier N (2009) Dual symbiosis of the vent shrimp Rimicaris exoculata with filamentous gamma- and epsilonproteobacteria at four Mid-Atlantic Ridge hydrothermal vent fields. *Environmental Microbiology*, **12**, 2204–2218.

Polz MF, Felbeck H, Novak R, Nebelsick M, Ott JA (1992) Chemoautotrophic, sulfur-oxidizing symbiotic bacteria on marine nematodes: morphological and biochemical characterization. *Microbial Ecology*, **24**, 313–329.

Ponsard J, Cambon-Bonavita M-A, Zbinden M *et al.* (2013) Inorganic carbon fixation by chemosynthetic ectosymbionts and nutritional transfers to the hydrothermal vent host-shrimp *Rimicaris exoculata*. *The ISME Journal*, **7**, 96–109.

Rogers AD, Tyler PA, Connelly DP *et al.* (2012) The discovery of new deep-sea hydrothermal vent communities in the southern ocean and implications for biogeography. *PLoS Biology*, **10**, e1001234.

Shin SC, Kim S-H, You H *et al.* (2011) *Drosophila* microbiome modulates host developmental and metabolic homeostasis via insulin signaling. *Science*, **334**, 670–674.

Steedman HF (1957) Polyester wax: a new ribboning embedding medium for histology. *Nature*, **179**, 1345.

Suzuki Y, Suzuki M, Tsuchida S *et al.* (2009) Molecular investigations of the stalked barnacle *Volcanolepas osheai* and the epibiotic bacteria from the Brothers Caldera, Kermadec Arc, New Zealand. *Marine Biological Association of the UK*, **89**, 727–733.

Tanaka N, Romanenko LA, Lino T, Frolova GM, Mikhailov VV (2011) Cocleimonas flava gen nov, a gammaproteobacterium isolated from sand snail (*Umbonium costatum*). *International Journal of Systematic and Evolutionary Microbiology*, **61**, 412–416.

Thurber AR, Jones WJ, Schnabel K (2011) Dancing for food in the Deep Sea: bacterial farming by a new species of yeti crab. *PLoS ONE*, **6**, e26243.

Tsuchida S, Suzuki Y, Fujiwara Y *et al.* (2011) Epibiotic association between filamentous bacteria and the vent-associated galatheid crab, *Shinkaia crosnieri* (Decapoda: Anomura). *Marine Biological Association of the UK*, **91**, 23–32.

Van Dover CL, Fry B, Grassle JF, Humphris S, Rona PA (1988) Feeding biology of the shrimp *Rimicaris exoculata* at hydrothermal vents on the Mid-Atlantic Ridge. *Marine Biology*, **98**, 209–216.

Watsuji T, Nakagawa S, Tsuchida S *et al.* (2010) Diversity and function of epibiotic microbial communities on the galatheid crab, *Shinkaia crosnieri*. *Microbes Environment*, **25**, 288–294.

Wernegreen JJ (2002) Genome evolution in bacterial endosymbionts of insects. *Nature Reviews Genetics*, **3**, 850–861.

Zbinden M, Shillito B, Le Bris N *et al.* (2008) New insights on the metabolic diversity among the epibiotic microbial community of the hydrothermal shrimp *Rimicaris exoculata*. *Journal of Experimental Marine Biology and Ecology*, **359**, 131–140.

S.K.G. collected samples, followed up on all data collection and results gathering, and wrote the final version of the manuscript. A.G. performed the initial DNA extractions, clone libraries, and generated tRFLP results for all 2009 samples. W.J.J. performed 16S rRNA barcoding and bioinformatic data analysis. N.M.M. performed FISH microscopy and contributed to figure construction. R.I.S. performed dissections of the adult crab, followed by DNA extraction of body regions, and juveniles from 2010, as well as tRFLP analysis and contribution to the results section.

Data accessibility

Pyrotag and tRFLP and data are supplied in the online supplemental materials.

Raw pyrotag reads are available from the Dryad Digital Repository: http://dx.doi.org/10.5061/dryad.6pd36] or by request from the author.

Supporting information

Additional supporting information may be found in the online version of this article.

Fig. S1 Juvenile specimens of *Kiwa puravida* used in this study. All scale bars, 1 mm.

Fig. S2 Relative abundance, for each of the common operational taxonomic units (based on 97% similarity in the 16S rRNA gene), obtained via pyrosequencing from *Kiwa puravida* crabs and eggs in this study.

Fig. S3 Principal component analysis (PCA) of relative taxon abundance, at the family-level, for 14 samples of *Kiwa puravida*, obtained by 16S rRNA pyrosequencing (same data as in Table S2, Supporting information).

Table S1 Fingerprinting pattern, by terminal restriction fragment length polymorphism analysis (T-RFLP) of the 16S rRNA gene, of the bacterial community for fourteen body regions of *Kiwa puravida* (as a % of the total signal).

Table S2 Phylogenetic classification, to the family level, for the pyrosequencing analysis of the 16S rRNA gene, obtained from *Kiwa puravida* crabs and eggs in this study, based on the Greengenes taxon assignments.

Table S3 Bacterial community diversity estimations, based on 16S rRNA pyrosequencing analysis using two different primer sets, for eggs and a juvenile specimen of *Kiwa puravida* from the Costa Rica margin.